



OPEN ACCESS

EDITED BY

Kwadwo Antwi-Fordjour,
Samford University, United States

REVIEWED BY

Anthony O'Hare,
University of Stirling, United Kingdom
Ndolane Sene,
Cheikh Anta Diop University, Senegal

*CORRESPONDENCE

Haileyesus Tessema
✉ hailsa.tessema@gmail.com

RECEIVED 01 November 2024

ACCEPTED 18 June 2025

PUBLISHED 29 July 2025

CITATION

Tessema H, Zemenu Y, Bizualem E and
Teshome G (2025) Improving immunization
initiatives in the dynamics of a typhoid fever
transmission model with environmental
bacteria concentration.
Front. Appl. Math. Stat. 11:1521177.
doi: 10.3389/fams.2025.1521177

COPYRIGHT

© 2025 Tessema, Zemenu, Bizualem and
Teshome. This is an open-access article
distributed under the terms of the [Creative
Commons Attribution License \(CC BY\)](#). The
use, distribution or reproduction in other
forums is permitted, provided the original
author(s) and the copyright owner(s) are
credited and that the original publication in
this journal is cited, in accordance with
accepted academic practice. No use,
distribution or reproduction is permitted
which does not comply with these terms.

Improving immunization initiatives in the dynamics of a typhoid fever transmission model with environmental bacteria concentration

Haileyesus Tessema^{1*}, Yimer Zemenu¹, Endlkachew Bizualem²
and Getachew Teshome³

¹Department of Mathematics, University of Gondar, Gondar, Ethiopia, ²Department of Biology, University of Gondar, Gondar, Ethiopia, ³Department of Mathematics, Haramaya University, Haramaya, Deri Dawa, Ethiopia

Typhoid fever is a potentially fatal disease and endemic to most parts of the world. It is a serious worldwide health issue, especially in developing countries, and is typically spread via contaminated food, water, or drink. This work introduced an SIVR-B model to explore and predict the dynamics of typhoid disease in a community. The effective reproduction number (R_{Eff}) of the model is calculated by manipulating the next-generation method. Then, after we computed the Typhoid fever-free equilibrium and the typhoid fever persistence equilibrium points, we demonstrated the global asymptotic stability of the equilibria. The bifurcation analysis demonstrated that the formulated typhoid model exhibits a forward bifurcation at $R_{Eff} = 1$. Further, the sensitivity of parameters is performed using normalized forward sensitivity analysis and demonstrated using numerical simulation. The work demonstrated that higher typhoid vaccination rates have a pronounced effect on lowering disease transmission. From the results, we recommended policymakers and government stakeholders should enhance immunization efforts to effectively address the dynamics of typhoid fever transmission. In addition to improving vaccination efficacy, the research work recommends reducing poor drainage systems and improving water quality to reduce the infection number.

KEYWORDS

typhoid fever, compartmental model, effective reproduction number, equilibrium points, stability analysis, numerical simulation

1 Introduction

The bacteria *Salmonella* (*S. typhi*) is the main cause of typhoid fever, a potentially devastating infection that is endemic to most parts of the world and only transmitted in humans [1]. Approximately 10–20 million new cases of typhoid fever are reported worldwide each year, with over a quarter of a million fatalities, primarily in Africa [2, 3], and this shows that the disease is still a serious challenge to global public health [4].

In areas with inadequate sanitation, typhoid fever can spread rapidly and result in a mass infection when individuals drink or eat food contaminated by an infected person's excrement [5, 6]. Inadequate sanitation systems and poor water quality, which facilitate the spread of infectious agents, are major contributors to the significant rise in illness rates,

especially in developing nations [3, 7, 8]. The hallmarks of *Salmonella* gastroenteritis include cramping in the abdomen, diarrhea (often with blood tinges), and occasionally nausea and vomiting. *Salmonella* bacteria are numerous and hardy, and they can survive for months in water and weeks in a dry environment [4, 9].

Despite being curable, typhoid fever is becoming increasingly difficult to eradicate due to growing resistance to various medications [4]. The lack of globally supported typhoid immunization campaigns has also been attributed to the effectiveness of drugs and the prior lack of a long-acting infant vaccine [10]. Although there are typhoid fever vaccines, their effectiveness is only partially guaranteed [4, 10].

Infectious disease mathematical modeling can be used as a tool to help public health policymakers understand the transmission dynamics of communicable diseases. The transmission of typhoid disease was studied by several researchers using various models. Among these researchers, Chamuchi et al. [11] aimed to simulate the transmission of typhoid disease by developing and examining the effects of carrier effects, diagnostics, and health education on the control of typhoid carriers in Kenya considering the SIICR Model. From their numerical result, they concluded that reducing typhoid carriers by 9.5% could assist the Kisii county government in Kenya achieve a typhoid-free status by 2030.

Protection, Susceptible, Infected, and Treated (PSIT) is the type of mathematical model proposed and examined by Akinyi et al. [12]. The researchers Edward and Nyerere [13] developed a mathematical model for typhoid fever to assess the effects of education campaigns, vaccination, and treatment on controlling the transmission dynamics of typhoid fever in a Tanzanian community. They investigated the impact of screening and treatment on the dynamics of each subpopulation through numerical simulations. The research undertaken by Peter et al. [5], presented an SI_cIR type model with perfect vaccination to study the transmission dynamics of typhoid fever diseases in a population. The results revealed that the transmission of typhoid fever largely depends on the contact rate with infected individuals within a population. They recommended that timely detection and early treatment could reduce the infection rate.

A deterministic mathematical model of typhoid fever incorporating unprotected humans was formulated by Karunditu et al. [14]. They concluded that the disease's spread depends on the number of unprotected individuals and other factors. Wameko et al. [15] investigated the dynamics of typhoid disease in a community using a deterministic model. Their numerical simulation results revealed that applying preventive measures has a significant impact on minimizing the incidence of the disease. If all intervention strategies are implemented, the disease will be eradicated in a short period of time. Nyaber et al. [16] proposed a mathematical model for typhoid transmission that analyzes the impact of treating infected individuals on the dynamics of the disease. They considered a model that consists of a human population and pathogen population. The findings of their work indicated that effective treatment is sufficient to eradicate typhoid fever. The research work done by Jan, Rashid

et al. [17], formulated an epidemic mathematical model for typhoid fever that incorporated vaccination and carriers using the Caputo-Fabrizio operator. They demonstrated the impact of fractional order and other parameters on the dynamics of typhoid fever.

Although the studies mentioned above have provided significant insights into the dynamics of typhoid fever, none have specifically examined its transmission dynamics while incorporating the impact of vaccination interventions alongside bacterial concentrations in the environment. Therefore, this study aims to fill this gap by investigating an issue that has received limited attention in previous research. Hence, the objective of this research is to analyze the interactions among vaccination efforts, environmental bacterial presence, and the transmission of typhoid fever, with the aim of providing a more comprehensive understanding of how these factors influence the spread of the disease.

2 Baseline model assumptions and formulation

In this section, the human and bacteria population are considered in the model construction. At time t the human population is grouped into four disjoint subclasses: Susceptible (S), Infected (I), Vaccinated (V), and Recovered (R).

2.1 Model assumptions

- I The population is uniform and mixes homogeneously,
- II Recruited newborns who received the vaccine join the Vaccinated class, but recruited newborns who have not received vaccine join the Susceptible class,
- III Susceptible individuals decrease due to consuming food or water contaminated with *S. typhi* that is able to transmit the disease,
- IV The vaccination given is not a perfect vaccine.

Individuals are recruited into the population at a rate π , with a fraction p vaccinated and the remaining $(1 - p)$ remaining susceptible. These susceptible individuals are vaccinated at a rate δ .

When susceptible people consume food or water contaminated with *Salmonella* bacterium, they contract the bacteria that causes typhoid fever $\lambda = \frac{\beta B}{K+B}$, where $B(t)$ is the bacteria in the environment, K is the *Salmonella* bacteria concentration in food or water, and β is the ingestion rate of *Salmonella*. The infected subclass increases *S. typhi* bacteria in the environment by human waste contamination rate η . After receiving treatment, members of the infected subclass can join the recovered subclass at a rate of ε . Individuals from the vaccinated class also contribute to the recovered subclass at a rate of ϕ . The human population assumed μ as the natural death rate, and the infective class die at an induced death rate ω , and μ_b is the decay rate of *S. typhi* bacteria from the environment. We consider that vaccinated individuals can become infected at a rate of $\theta\lambda$ due to vaccine inefficacy, providing only partial protection. The

TABLE 1 Description of parameters in the Model (1) and their values.

Parameter	Description	Values	Units	Source
β	Ingestion rate of <i>Salmonella</i>	0.36	Month^{-1}	Tillahun G. T. et al., 2017
θ	Probability of vaccinated joining infected	0.12	Month^{-1}	Assumed
ε	Recovery rate of infectious individuals	0.032	Month^{-1}	Assumed
η	Rate of infected population increasing the concentration bacteria environment	0.32	$\text{Cells } \text{Ml}^{-1} \text{ Human}^{-1} \text{Month}^{-1}$	Assumed
μ_b	Decay rate of <i>Salmonella</i> bacteria	0.138	Month^{-1}	Assumed
ω	Typhoid-induced death rate	0.0264	Month^{-1}	Assumed
μ	Natural mortality rate of human population	0.0098	Month^{-1}	Tillahun G. T. et al., 2017
σ	The rate at which vaccinated become susceptible	0.132	Month^{-1}	Choe, K., Whittington, D., and Lauria, D. T. (2019).
δ	The rate at which susceptible become vaccinated	0.3	Month^{-1}	Nyerere, N., Mpeshe, S. C., and Edward, S. (2018).
φ	Recovery rate of vaccinated by natural immunity	0.08	Month^{-1}	Nyerere, N., Mpeshe, S. C., and Edward, S. (2018).
p	Proportion of births with successful vaccination	0.2	$\text{Humans } \text{Month}^{-1}$	Mushayabasa, S. (2013).
π	Recruitment rate of susceptible individuals	40	$\text{Human } \text{Month}^{-1}$	Tillahun G. T. et al., 2017
K	Concentration of bacteria in food or water	200	$\text{Cells } \text{Ml}^{-1} \text{ Month}^{-1}$	Gordon, M. A., et al. (2008).

broken line drawn from B to S indicates the contact between susceptible people and food or water contaminated with *Salmonella* bacterium. The descriptions of the model parameters are listed in Table 1.

The model comprises the following system of differential equations based on the presumptions and the compartmental diagram in Figure 1 with initial conditions $S(0) > 0, V(0) \geq 0, I(0) \geq 0, R(0) \geq 0, B(0) \geq 0$.

$$\left. \begin{aligned} \frac{dS}{dt} &= (1-p)\pi + \sigma V - \lambda S - (\delta + \mu)S \\ \frac{dV}{dt} &= p\pi + \delta S - \theta\lambda V - (\sigma + \varphi + \mu)V \\ \frac{dI}{dt} &= \lambda S + \theta\lambda V - (\varepsilon + \omega + \mu)I \\ \frac{dR}{dt} &= \varphi V + \varepsilon I - \mu R \\ \frac{dB}{dt} &= \eta I - \mu_b B \end{aligned} \right\} \quad (1)$$

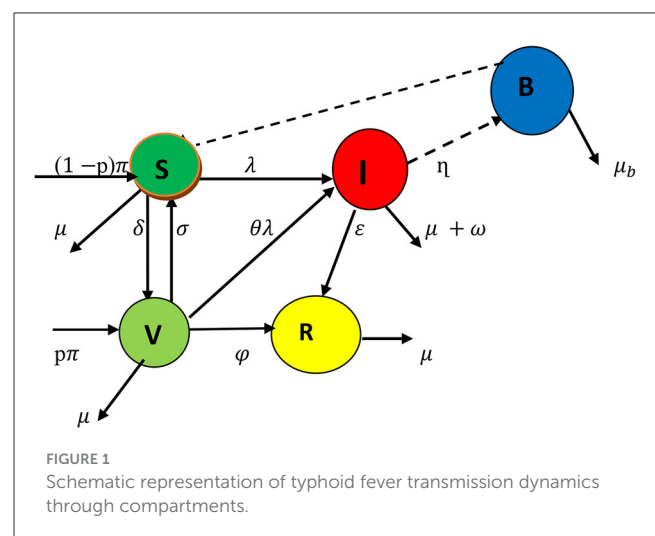
3 Model analysis

3.1 Invariant region and positivity of the solutions

Theorem 3.1: The model's possible solutions are all uniformly bounded within the proper subset $\Omega = \Omega_H \times \Omega_B$ where $\Omega_H = \{(S, V, I, R) \in \mathbb{R}_+^4 : N(t) \leq \frac{\pi}{u}\}$ is a subset for human population and $\Omega_B = \{B \in \mathbb{R}_+ : B \leq n \frac{\pi}{u}\}$ is a subset associated with environmental bacterial infections.

Proof: $N = S + V + I + R$ yields the entire human population $N(t)$ under the initial conditions $N(0) = N_0 = S_0 + V_0 + I_0 + R_0$ and $B(0) = B_0$ for *S.typhi* bacteria in the environment. Establishing a differentiation of N and with respect to time (t), we obtain

$$\frac{dN}{dt} = \frac{dS}{dt} + \frac{dV}{dt} + \frac{dI}{dt} + \frac{dR}{dt} \quad (2)$$



Substituting Equation 1 in place of Equation 2 and assuming no disease-induced death rate (i.e making $\omega = 0$), we have

$$\frac{dN}{dt} \leq \pi - u N(t) \quad (3)$$

Rearranging and integrating both sides of Equation 3, we get

$$N(t) \leq \frac{\pi}{u} + \left(N_0 - \frac{\pi}{u}\right) e^{-ut} \quad (4)$$

When time moves to ∞ in Equation 4, $N(t)$ converges to π/u ; this indicates that there are feasible model solutions for the local population.

$$\Omega_H = \{(S, V, I, R) \in \mathbb{R}_+^4 : N(t) \leq \frac{\pi}{u}\} \quad (5)$$

For bacteria environment since $N(t) \leq \pi/u$, it means that $I \leq \pi/u$. We have from the last Equation 1 that

$$\frac{dB}{dt} = \eta I - \mu_b B \leq \eta N - \mu_b B \leq \eta \frac{\pi}{\mu} - \mu_b B \quad (6)$$

Evaluating Equation 6 with $B(0) = B_0$ as a stating condition yields

$$B(t) \leq \frac{\eta \pi}{\mu \mu_b} + \left(B_0 - \frac{\eta \pi}{\mu \mu_b} \right) e^{-\mu_b t} \quad (7)$$

As t tends to infinity, Equation 7 becomes $B(t) \leq \frac{\eta \pi}{\mu}$. Therefore, the feasible solution of the bacteria population enters the region

$$\Omega_B = \left\{ B \in R_+ : B \leq \frac{\eta \pi}{\mu} \right\} \quad (8)$$

Therefore, from Equations 5, 8 the feasible region of the model is given by

$$\Omega = \Omega_H \times \Omega_B = \left\{ (S, V, I, R) \in R_+^4 : N(t) \leq \frac{\pi}{\mu}, B \in R_+ : B \leq \frac{\eta \pi}{\mu} \right\}$$

Theorem 3.2: Let $\Omega = \{ (S, V, I, R, B) \in R_+^5 : S(0) > 0, V(0) \geq 0, I(0) \geq 0, R(0) \geq 0, B(0) \geq 0 \}$ then the solution $\{ S, V, I, R, B \}$ are positive for all $t \geq 0$.

Proof: From the fifth equation of model (1)

$$\frac{dB}{dt} \geq -B \mu_b \quad (9)$$

By using comparison theorem, Equation 9 is solved as, we get $(t) \geq e^{-\mu_b t} C$,

$$B(t) \geq B(0) e^{-\mu_b t} \geq 0, \text{ where } B(0) = e^C \text{ att} = 0$$

From the first equation of model (1), we have

$$\frac{dS}{dt} \geq -\left(\frac{\beta B}{K+B} + (\delta + \mu) \right) S \quad (10)$$

By comparison theorem, integrating Equation 10 with initial conditions $S(0) = S_0$ yields

$$S(t) \geq S_0 e^{-\left(\frac{\beta B}{K+B} + (\delta + \mu) \right) t} \geq 0$$

After substituting the solution of $B(t)$, we get

$$S(t) \geq S_0 e^{-\left(\frac{\beta B(0)}{K+B(0)} e^{-\mu_b t} + (\delta + \mu) \right) t} \geq 0$$

Similarly, we can prove the positivity of the other variables as

$$\begin{aligned} V(t) &\geq V_0 e^{-\left(\frac{\theta \beta B(0)}{K+B(0)} e^{-\mu_b t} + (\sigma + \varphi + \mu) \right) t} \geq 0, I(t) \\ &\geq I(0) e^{-(\varepsilon + \eta + \omega + \mu)t} \geq 0 \end{aligned}$$

and $(t) \geq R(0) e^{-\mu t} \geq 0$. Thus $S(t)$, $V(t)$, $I(t)$, $R(t)$, and $B(t)$ are positive for all $t \geq 0$

3.2 Typhoid fever-free equilibrium

We denote the typhoid fever-free equilibrium by E^0 . By setting the right-hand side of the equations in system (1) to zero and simultaneously solving for the uninfected compartments S , V , and R , we obtain the typhoid fever-free equilibrium as:

$$E^0 = (S^0, V^0, I^0, R^0, B^0) = \left(\frac{\pi k_3}{k_4}, \frac{\pi k_5}{k_6}, 0, \frac{\phi \pi k_5}{\mu k_6}, 0 \right) \quad (11)$$

where $k_1 = \delta + \mu$, $k_2 = \sigma + \varphi + \mu$, $k_3 = -k_2(1-p) - p\sigma$, $k_4 = \sigma\delta - k_2k_1$;

$$k_5 = -k_4(1-p) - k_1k_3 \text{ and } k_6 = \sigma k_4$$

3.3 Effective reproduction number

When an infected person enters a vaccinated community, the average number of secondary cases produced is known as the effective reproduction number R_{Eff} . It is computed using the next-generation matrix approach, J [18, 19]. Using the principle

$$F = \begin{Bmatrix} \frac{\beta BS}{K+B} + \frac{\theta \beta BV}{K+B} \\ 0 \end{Bmatrix} \text{ and } V = \begin{Bmatrix} (\varepsilon + \omega + \mu)I \\ -\eta I + \mu_b B \end{Bmatrix} \quad (12)$$

Then, from Equation 12, the Jacobian matrices evaluated at the FFEP are obtained as:

$$f = \begin{bmatrix} 0 & \frac{\beta(S^0 + \theta V^0)}{K} \\ 0 & 0 \end{bmatrix}, \quad v = \begin{bmatrix} \varepsilon + \omega + \mu & 0 \\ -\eta & \mu_b \end{bmatrix}$$

Computing the inverse of v , we get

$$\begin{aligned} v^{-1} &= \frac{1}{\det(v)} \text{Adjoint}(v) = \frac{1}{\mu_b(\varepsilon + \omega + \mu)} \begin{bmatrix} \mu_b & 0 \\ \eta & \varepsilon + \omega + \mu \end{bmatrix} \\ &= \begin{bmatrix} \frac{1}{(\varepsilon + \omega + \mu)} & 0 \\ \frac{\eta}{\mu_b(\varepsilon + \omega + \mu)} & \frac{1}{\mu_b} \end{bmatrix} \end{aligned}$$

Then using the principle, the next-generation matrix is given by

$$\begin{aligned} G = f v^{-1} &= \begin{bmatrix} 0 & \frac{\beta(S^0 + \theta V^0)}{K} \\ 0 & 0 \end{bmatrix} \begin{bmatrix} \frac{1}{(\varepsilon + \omega + \mu)} & 0 \\ \frac{\eta}{\mu_b(\varepsilon + \omega + \mu)} & \frac{1}{\mu_b} \end{bmatrix} \\ &= \begin{bmatrix} \frac{\beta \eta (S^0 + \theta V^0)}{K \mu_b (\varepsilon + \omega + \mu)} & \frac{\beta (S^0 + \theta V^0)}{K \mu_b} \\ 0 & 0 \end{bmatrix} \end{aligned}$$

The eigenvalue of a matrix G determined by $\det(G - \lambda I) = 0$ and the dominant eigenvalue becomes the effective reproduction number of the model. Hence,

$$R_{\text{Eff}} = \frac{\beta \eta \pi (\delta \theta + \sigma + \varphi + u) (1-p) + p(\theta(\delta + u) + \sigma)}{k \mu_b (\varepsilon + \omega + \mu) [\mu(\mu + \delta + \varphi + u) + \delta \varphi]}$$

3.4 Local stability typhoid fever-free equilibrium point

Theorem 3.3: The typhoid fever-free equilibrium E^0 of the model (1) is locally asymptotically stable (LAS) if $R_{\text{Eff}} < 1$, otherwise it is unstable.

Proof: The Jacobian matrix of the model in Equation 1 is given by

$$J = \begin{bmatrix} \frac{\beta B}{K+B} - (\delta + \mu) & \sigma & 0 & 0 & \frac{-\beta S}{K+B} + \frac{\beta B}{(K+B)^2} \\ \delta & \frac{\theta \beta B}{K+B} - (\sigma + \varphi + \mu) & 0 & 0 & -\frac{\theta \beta V}{K+B} + \frac{\theta \beta BV}{(K+B)^2} \\ \frac{\beta B}{K+B} & \frac{\theta \beta B}{K+B} & -(\varepsilon + \omega + \mu) & 0 & \frac{\beta S}{K+B} - \frac{\beta BS}{(K+B)^2} + \frac{\theta \beta BV}{K+B} - \frac{\theta \beta BV}{(K+B)^2} \\ 0 & \varphi & \varepsilon & -u & 0 \\ 0 & 0 & \eta & 0 & -\mu_b \end{bmatrix}$$

If we evaluated at the typhoid fever-free equilibrium point E^0 , we get

$$J = \begin{bmatrix} -(\delta + \mu) & \sigma & 0 & 0 & \frac{-\beta S^0}{K} \\ \delta & -(\sigma + \varphi + \mu) & 0 & 0 & -\frac{\theta \beta V^0}{K} \\ 0 & 0 & -(\varepsilon + \omega + \mu) & 0 & \frac{\beta S^0}{K} + \frac{\theta \beta V^0}{K} \\ 0 & \varphi & \varepsilon & -\mu & 0 \\ 0 & 0 & \eta & 0 & -\mu_b \end{bmatrix} \quad (13)$$

To make the proof more clarified, the Jacobian is block-triangular; this allows us to partition it and compute eigenvalues separately. Let us use submatrix, as infected and healthy:

Healthy states (S,V,R):

$$J_1 = \begin{bmatrix} -(\delta + \mu) & \sigma & 0 \\ \delta & -(\sigma + \varphi + \mu) & 0 \\ 0 & 0 & -\mu \end{bmatrix}$$

Infected states (I,B):

$$J_2 = \begin{bmatrix} -(\varepsilon + \omega + \mu) & \frac{\beta S^0}{K} + \frac{\theta \beta V^0}{K} \\ \eta & -\mu_b \end{bmatrix}$$

Since J_1 is a lower triangular, the eigenvalues are its diagonal entries:

$$(-u - \lambda) \begin{vmatrix} -(\delta + \mu) - \lambda & \sigma \\ \delta & (\sigma + \varphi + \mu) - \lambda \end{vmatrix} = 0$$

The first eigenvalue is $-u = \lambda_1$ and the other eigenvalues are obtained from the characteristic equation given by

$$(-(\delta + \mu) - \lambda)(-(\sigma + \varphi + \mu) - \lambda) - \sigma \delta = 0. \\ \lambda^2 + A\lambda + B = 0$$

where

$$A = \delta + \mu + \sigma + \varphi + \mu > 0, \\ B = \delta \sigma + \delta \varphi + \delta \mu + \mu \sigma + \mu \varphi + \mu^2 - \sigma \delta = \delta \varphi + \delta \mu + \mu \sigma + \mu \varphi + \mu^2 > 0$$

Hence the eigenvalues of the matrix J_1 are negative from the Hurwitz criterion.

The eigenvalues of J_2 determine the stability of the infected states. The characteristic equation is:

$$\begin{vmatrix} -(\varepsilon + \omega + \mu) - \lambda & \frac{\beta S^0}{K} + \frac{\theta \beta V^0}{K} \\ \eta & -\mu_b - \lambda \end{vmatrix} = 0$$

The corresponding characteristic equation is given by

$$\lambda^2 + (\varepsilon + \mu + \omega + \mu_b) \lambda + (\varepsilon + \mu + \omega) \mu_b - \frac{\beta \eta (S^0 + \theta V^0)}{K} = 0 \quad (14)$$

where

$$a_1 = \varepsilon + \mu + \omega + \mu_b > 0, \\ a_2 = (\varepsilon + \mu + \omega) \mu_b - \frac{\beta \eta (S^0 + \theta V^0)}{K}, \\ = (\varepsilon + \mu + \omega) \mu_b \left(1 - \frac{\beta \eta (S^0 + \theta V^0)}{K \mu_b (\varepsilon + \mu + \omega)} \right) \\ = (\varepsilon + \mu + \omega) \mu_b (1 - R_{\text{Eff}}) > 0$$

Therefore, the disease-free equilibrium point is LAS whenever $R_{\text{Eff}} < 1$.

3.5 Global stability of typhoid fever-free equilibrium

We utilized the Castillo-Chávez et al. [20] technique to show the globally stability of typhoid fever-free equilibrium as it used by Alemneh and Alemu [21]. The Castillo-Chávez et al. [20] method divides the population into two as

$$\frac{dx}{dt} = F_1(x, z), \\ \frac{dz}{dt} = F_2(x, z), F_2(x, 0) = 0 \quad (15)$$

$x \in \mathbb{R}^3$ shows the number of uninfected individuals (susceptible, vaccinated, and recovered) while $z \in \mathbb{R}^2$ is the number of infected human individuals and bacteria in the environment. Let the typhoid fever-free equilibrium be denoted by $(x^0, 0)$. The two basic axioms that guarantee the global stability of typhoid fever-free equilibrium are:

H_1 : For $\frac{dx}{dt} = F_1(x, 0)$, x^0 is globally asymptotically stable.

H_2 : $F_2(x, z) = Az - \overline{F}_2(x, z)$ where $\overline{F}_2(x, z) \geq 0$ for $(x, z) \in \Omega$ and the

matrix $A = D_z F_2(x^0, 0)$ denotes an M-matrix.

Theorem 3.4: The typhoid fever-free equilibrium point of the model (1) is globally asymptotically stable (GAS) if the system in Equation 15 satisfies the axioms (H_1) and (H_2) for $R_{\text{Eff}} < 1$ otherwise unstable.

Proof: Let $x = (S(t), V(t), R(t))$ and $z = (I(t), B(t))$ represent the number of uninfected and infected individuals, respectively. Define $E^0 = (x^0, 0)$, $x^0 = (\frac{\pi k_3}{k_4}, \frac{\pi k_5}{k_6}, \frac{\phi}{\pi} k_5 \mu k_6)$.

$$F_1(x, z) = \begin{pmatrix} (1-p) \pi + \sigma V - \frac{\beta B}{K+B} S - (\delta + \mu) S \\ p \pi + \delta S - \frac{\theta \beta B}{K+B} V - (\sigma + \varphi + \mu) V \\ \varphi V + \varepsilon I - \mu R \end{pmatrix} \quad (16)$$

The reduced system according to the condition H_1 : becomes

$$\begin{aligned}\frac{dS}{dt} &= (1-p)\pi + \sigma V - (\delta + \mu)S \\ \frac{dV}{dt} &= p\pi + \delta S - (\sigma + \varphi + \mu)V \\ \frac{dR}{dt} &= \varphi V - \mu R\end{aligned}\quad (17)$$

Solving Equation 17 one by one, we have

$$S(t) = \frac{[(1-p)\pi + \sigma V^0]}{(\delta + \mu)} + \frac{c}{e^{(\delta + \mu)t}} \quad (18)$$

From Equation 18, as t approaches ∞ , $\frac{c}{e^{(\delta + \mu)t}}$ approaches to zero.

$$\text{Substitute } V^0 = \frac{\pi(\sigma + \mu P)}{\sigma(\varphi + \mu) + \mu(\sigma + \varphi + \mu)} \text{ we get } S(t) = \left(\frac{(1-p)\pi + \sigma \left(\frac{\pi(\sigma + \mu P)}{\delta(\varphi + \mu) + \mu(\sigma + \varphi + \mu)} \right)}{(\delta + \mu)} \right)$$

$$\left(\frac{(1-p)\pi + \sigma \left(\frac{\pi(\sigma + \mu P)}{\delta(\varphi + \mu) + \mu(\sigma + \varphi + \mu)} \right)}{(\delta + \mu)} \right) = \frac{\pi(\sigma + (\varphi + \mu)(1-p))}{\delta(\varphi + \mu) + \mu(\sigma + \varphi + \mu)} = S^0$$

Similarly, we show for R and V

$$\begin{aligned}\lim_{t \rightarrow \infty} [p\pi + \delta \left(\frac{\pi(\sigma + (\varphi + \mu)(1-p))}{\delta(\varphi + \mu) + \mu(\sigma + \varphi + \mu)} \right)] + \frac{C}{e^{(\sigma + \varphi + \mu)t}} \\ = V^0 \text{ and } \lim_{t \rightarrow \infty} \frac{\varphi \pi(\sigma + \mu P)}{\mu(\delta(\varphi + \mu) + \mu(\sigma + \varphi + \mu))} + \frac{c}{e^{\mu t}} = R^0\end{aligned}$$

Therefore, as $t \rightarrow \infty$ $x(t) \rightarrow x^0$. Thus, $x^0 = (\frac{\pi k_3}{k_4}, \frac{\pi k_5}{k_6}, \frac{\phi \pi k_5}{\mu k_6})$ is globally asymptotically stable. Now to prove the second condition, we have

$$F_2(x, z) = \left(\frac{\frac{\beta B}{K+B}S + \frac{\theta \beta B}{K+B}V - (\varepsilon + \omega + \mu)I}{\eta I - \mu_b B} \right) \quad (19)$$

Using condition H_2 the matrix $A = D_z F_2(x, 0)$ of Equation 19, evaluated at typhoid fever-free equilibrium point given by

$$A = \begin{bmatrix} -(\varepsilon + \omega + \mu) & \frac{\beta K S^0}{K} + \frac{\theta \beta V^0}{K} \\ \eta & -\mu_b \end{bmatrix}$$

Hence from $\overline{F}_2(x, z) = AZ - F_2(x, z)$, we have

$$\overline{F}_2(x, z) = \begin{bmatrix} \beta B \left(\frac{S^0}{K} - \frac{S}{K+B} \right) + \beta B \left(\frac{V^0}{K} - \frac{V}{K+B} \right) \\ 0 \end{bmatrix}$$

Since $S^0 \geq S$, $V^0 \geq V$ and $\frac{1}{K} \geq \frac{1}{K+B}$, thus $\overline{F}_2(x, z) \geq 0$ $(x, z) \in \Omega$. Thus, H_1 : and H_2 : are satisfied, so, the typhoid fever-free equilibrium point E^0 is GAS. This result is also supported by the theorem 3.6 in Section 3.6.

3.6 Endemic equilibrium point

The endemic equilibrium point exists when $R_{Eff} > 1$. Let $E^1 = (S^*, V^*, I^*, R^*, B^*) \neq 0$ denote the endemic equilibrium of

model (1) and it is obtained by setting all the derivatives in model (1) to zero, i.e.,

$$\frac{dS}{dt} = \frac{dV}{dt} = \frac{dI}{dt} = \frac{dR}{dt} = \frac{dB}{dt} = 0$$

We obtained

$$\begin{aligned}V^* &= \frac{(\varepsilon + \omega + \mu)(k\mu_b + \eta I^*) - \beta \eta \pi}{\beta \eta (\sigma - (\varphi + \mu) + \mu \theta)}, \\ S^* &= \frac{(\varepsilon + \omega + \mu)(k\mu_b + \eta I^*) [\sigma - (\varphi + \mu)] - \beta \eta \pi}{\beta \eta (\sigma - (\varphi + \mu) + \mu \theta)},\end{aligned}$$

$$R^* = \frac{\varphi(\varepsilon + \omega + \mu)(k\mu_b + \eta I^*) - \varphi \beta \eta \pi + \beta \eta (\sigma - (\varphi + \mu) + \mu \theta) I^*}{\mu \beta \eta (\sigma - (\varphi + \mu) + \mu \theta)}, B^* = \frac{\eta}{\mu_b} I^*$$

Where I^* is the positive root of the following quadratic function

$$\eta^2 M T I^{*2} + Q I^* + L = 0 \quad (20)$$

with

$$\begin{aligned}M &= (\varepsilon + \omega + \mu), T = -\sigma \delta + \delta \varphi + \delta \mu + \mu \varphi + \mu^2 \\ Q &= \eta [(1-p)\pi r + \sigma \eta \beta \pi - r p - \delta k \mu_b \sigma M \delta k \mu_b M \\ &\quad + \delta k \mu_b \mu M - 2 \mu k \mu_b \sigma M + 2 k \mu_b \varphi M + 2 \mu^2 k \mu_b M \\ &\quad - \delta M k \mu_b \sigma + \delta \varphi M k \mu_b + \delta \varphi M k \mu_b + \delta \theta \beta \eta \pi - \mu M k \mu_b \sigma \\ &\quad + \mu \varphi M k \mu_b + \mu^2 M \mu_b + \mu M \eta] \\ L &= (1-p)\pi r k \mu_b + \delta k^2 \mu_b^2 M \mu \\ &\quad - \delta k \mu_b \beta \pi \eta + \sigma \eta M k \mu_b - \delta k^2 \mu_b^2 M \sigma + \delta k^2 \mu_b^2 M \varphi \\ &\quad + \delta k^2 \mu_b^2 M \mu - \delta k \mu_b \theta \beta \eta \pi - 2 \mu k^2 \mu_b^2 M \sigma \\ &\quad + 2 \mu k^2 \mu_b^2 M \varphi + 2 \mu^2 k^2 \mu_b^2 M + 2 \mu_b \beta \pi \eta \theta\end{aligned}$$

Theorem 3.5: For $R_{Eff} > 1$, there is a unique endemic equilibrium point and no endemic equilibrium elsewhere.

Proof: For the disease to be endemic $\frac{dI}{dt} > 0$, $\frac{dB}{dt} > 0$. Hence,

$$\begin{aligned}\frac{\beta B S}{K+B} + \frac{\theta \beta B}{K+B} V &> (\varepsilon + \omega + \mu) I \Rightarrow (\varepsilon + \omega + \mu) I \\ &< \frac{\beta B S}{K+B} + \frac{\theta \beta B}{K+B} V \\ \Rightarrow I &< \frac{\beta B S + \theta \beta B V}{(K+B)(\varepsilon + \omega + \mu)} \text{ and } \eta I > \mu_b B \Rightarrow \mu_b B \\ &< \eta I \Rightarrow B < \frac{\eta I}{\mu_b}, \\ \Rightarrow 1 &< \frac{\eta \beta S^0}{\mu_b (K+B^0)(\varepsilon + \omega + \mu)} \\ &\quad + \frac{\eta \theta \beta V^0}{\mu_b (K+B^0)(\varepsilon + \omega + \mu)}\end{aligned}\quad (21)$$

Since $B^0 \geq 0$, then Equation 22 is reduced to

$$1 < \frac{\eta \beta S^0 + \eta \theta \beta V^0}{\mu_b k (\varepsilon + \omega + \mu)} \Rightarrow 1 < R_{Eff} \text{ implies } R_{Eff} > 1$$

3.7 Local stability of EEP and bifurcation analysis

The local stability of the endemic equilibrium is established by demonstrating the existence of a forward bifurcation of the system using the center manifold technique, which is employed due to the mathematical difficulty of endemic equilibrium stability. A forward bifurcation indicates that the endemic equilibrium is locally asymptotically stable if $R_{Eff} > 1$ but near unity.

Using the approach of the center manifold theory [20, 22], we demonstrated the bifurcation analysis of the typhoid fever model in Equation 1. Let $\beta = \beta^*$ be a bifurcation parameter at $R_{Eff} = 1$, so that

$$\beta = \beta^* = \frac{k\mu_b(\varepsilon + \omega + \mu)[\mu(\delta + \varphi + \sigma + \mu) + \delta\varphi]}{\eta\pi(\delta\theta + \mu + \sigma + \varphi)(1 - p) + p(\theta(\delta + \mu) + \sigma)},$$

and we assume that $S = z_1$, $V = z_2$, $I = z_3$, $R = z_4$, $B = z_5$ and the model (1) is given by

$$\begin{cases} (1 - p)\pi + \sigma z_2 - \frac{\beta z_5 z_1}{K + z_5} - (\delta + \mu) z_1 = 0 \\ p\pi + \delta z_1 - \frac{\theta \beta z_5 z_2}{K + z_5} - (\sigma + \varphi + \mu) z_2 = 0 \\ \frac{\beta z_5 z_1}{K + z_5} + \frac{\theta \beta z_5 z_2}{K + z_5} - (\varepsilon + \omega + \mu) z_3 = 0 \\ \varphi z_2 + \varepsilon z_3 - \mu z_4 = 0 \\ \eta z_3 - \mu_b z_5 = 0 \end{cases} \quad (23)$$

The Jacobian matrix of the system [9] around the typhoid-free equilibrium point evaluated at $R_{Eff} = 1$ is

$$J = \begin{bmatrix} -(\delta + \mu) & \sigma & 0 & 0 & -\frac{\beta z_1^0}{k} \\ \delta & -(\sigma + \varphi + \mu) & 0 & 0 & -\frac{\theta \beta z_2^0}{k} \\ 0 & 0 & -(\varepsilon + \omega + \mu) & 0 & \frac{\beta z_1^0}{k} + \frac{\theta \beta z_2^0}{k} \\ 0 & \varphi & \varepsilon & -\mu & 0 \\ 0 & 0 & \eta & 0 & -\mu_b \end{bmatrix}$$

The right eigenvector $W = (w_1, w_2, w_3, w_4, w_5)^t$ associated with this simple zero eigenvalue can be obtained from $JW = 0$.

$$\begin{aligned} w_2 &= \left[\frac{\delta \beta z_1^0 + \theta \beta z_2^0 (\delta + \mu)}{k(\delta \sigma - (\delta + \mu)(\sigma + \varphi + \mu))} \right] w_5, \\ w_1 &= \left[\frac{\sigma \theta \beta z_2^0 + \beta z_1^0 (\sigma + \varphi + \mu)}{k(\delta \sigma - (\delta + \mu)(\sigma + \varphi + \mu))} \right] w_5, \\ w_3 &= \frac{\mu_b}{\eta} w_5, w_4 = \frac{1}{\mu \eta} \left[\frac{\phi x}{y} + \frac{\varepsilon \mu_b}{\eta} \right] w_5 \end{aligned}$$

where $x = \delta \beta z_1^0 + \theta \beta z_2^0 (\delta + \mu)$ and $y = k(\delta \sigma - (\delta + \mu)(\sigma + \varphi + \mu))$. The left eigenvector $= (v_1, v_2, v_3, v_4, v_5)^t$,

TABLE 2 Sensitivity indices of parameter values.

Parameter	Indices value	Parameter	indices value
π	1	μ	-0.2890018160
β	1	σ	0.5053949394
θ	0.1509327077	φ	0.5847016899
η	1	p	-0.07383019987
ε	-0.4692082111	ω	-0.3870967742
δ	-0.7753864479	K	-1
μ_b	-1		

associated with this simple zero eigenvalue, can be obtained from $VJ = 0$ and given by

$$v_1 = 0, v_2 = 0, v_4 = 0, v_3 > 0 \text{ and } v_5 = \frac{(\varepsilon + \eta + \omega + \mu)}{\eta} v_3$$

We do not require the derivative of f_1 , f_2 , and f_4 since the first, second, and fourth components of V are all zero. Additionally, since the expression for f_5 is linear, all its second-order partial derivatives are zero. From the derivatives the only ones that are non-zero are derivatives from f_3 and are listed below.

$$\begin{aligned} \frac{\partial^2 f_3(E^0)}{\partial z_2 \partial z_5} &= \frac{\partial^2 f_3(E^0)}{\partial z_5 \partial z_2} = \frac{\theta \beta}{k} \frac{\partial^2 f_3(E^0)}{\partial z_1 \partial z_5} = \frac{\partial^2 f_3(E^0)}{\partial z_5 \partial z_1} \\ &= \frac{\beta}{k} \text{ and } \frac{\partial^2 f_3(E^0)}{\partial z_5 \partial z_\beta} = \left(\frac{z_1^0}{k} + \frac{\theta z_2^0}{k} \right) \end{aligned}$$

The signs of the derived bifurcation coefficients a and b reflect the direction of the bifurcation at $R_{Eff} = 1$.

$$\begin{aligned} a &= \sum_{k,i,j=1}^5 v_k w_i w_j \frac{\partial^2 f_k}{\partial x_i \partial x_j} = -\frac{2v_3 w_5^2 \beta}{k^2} \\ &\left[\frac{\delta \theta \beta z_1^0 + \theta^2 \beta z_2^0 (\delta + \mu) + \sigma \theta \beta z_2^0 + \beta z_1^0 (\sigma + \varphi + \mu)}{((\varphi + \mu)(\delta + \mu) + \mu \sigma)} \right] < 0 \\ b &= \sum_{k,i=1}^5 v_k w_i \frac{\partial^2 f_k}{\partial x_i \partial x_\beta} = v_3 w_5 \frac{\partial^2 f_3(E^0)}{\partial z_5 \partial \beta} \\ &= v_3 w_5 \left(\frac{z_1^0}{k} + \frac{\theta z_2^0}{k} \right) > 0, \end{aligned}$$

Consequently, a supercritical bifurcation takes place in the model since the bifurcation coefficient, b , is inherently positive and a is negative. Thus, the theorem is inferred from the outcome.

Theorem 3.6. Whenever $R_{Eff} > 1$ but near unity, the following are true:

- The endemic equilibrium is locally asymptotically stable.
- The model illustrates forward bifurcation.
- The DFE point is globally asymptotically stable.

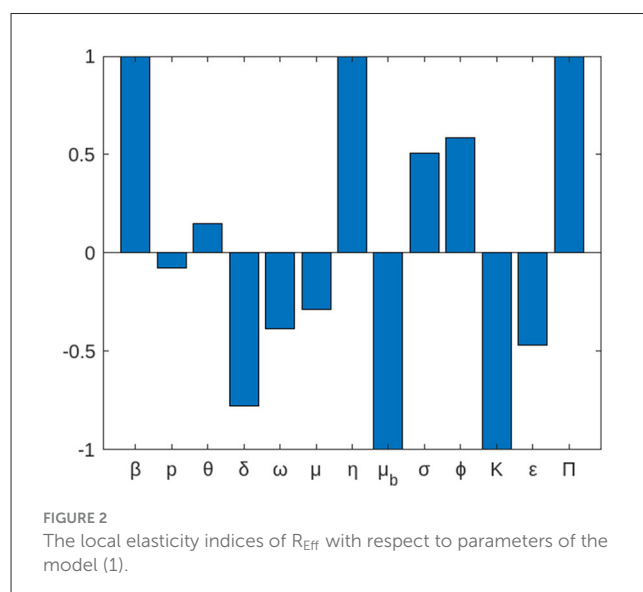


FIGURE 2

The local elasticity indices of R_{Eff} with respect to parameters of the model (1).

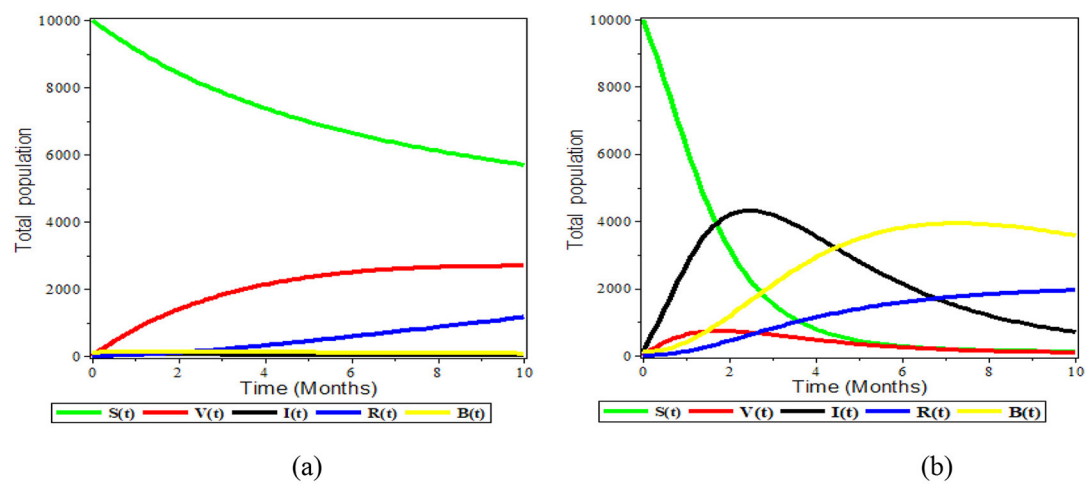


FIGURE 3
Graphical representation of the model (1) (a) left $R_{Eff} < 1$ and (b) right $R_{Eff} > 1$.

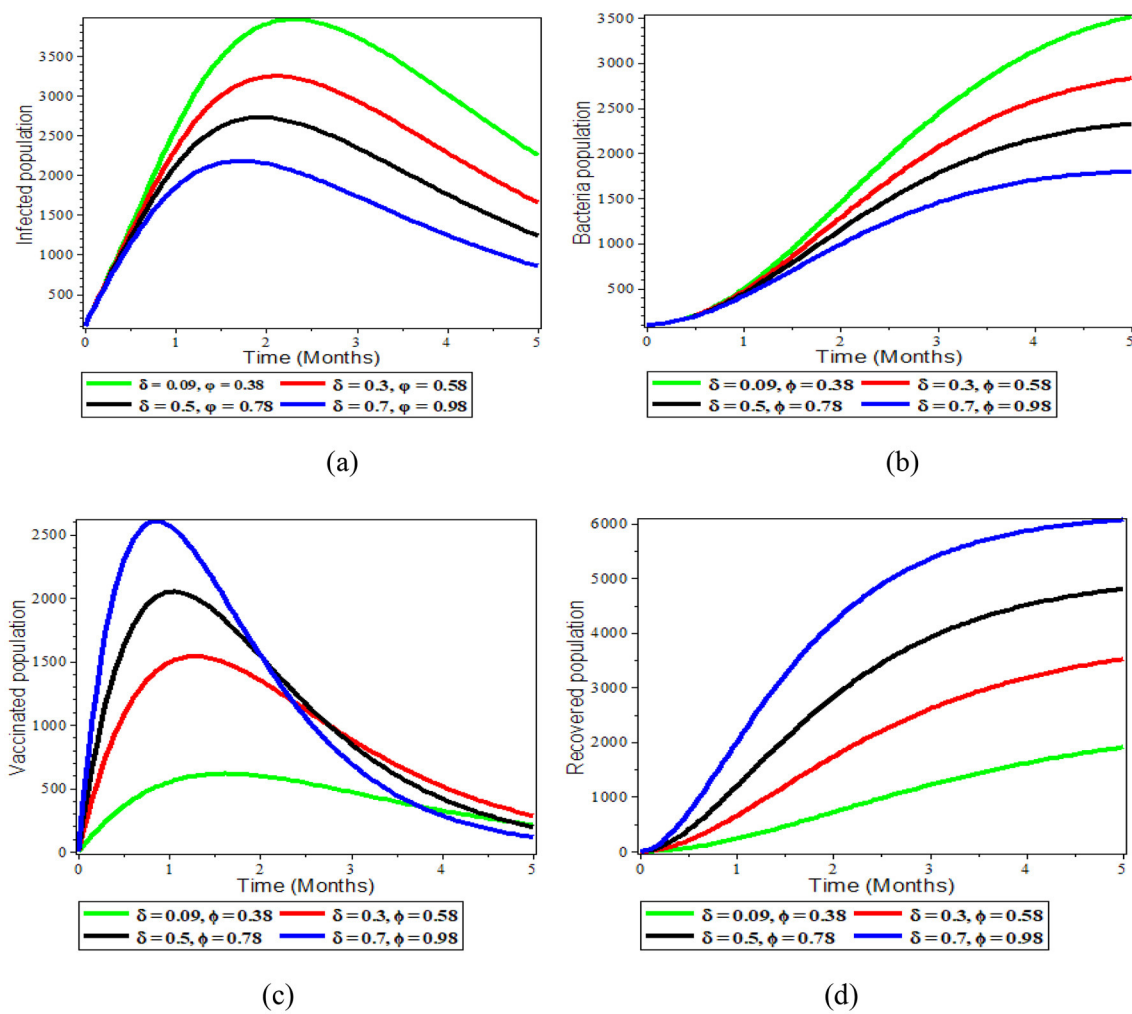


FIGURE 4
Graphs showing the sensitivity of model (1) varying δ and ϕ ; (a) Infected population; (b) Bacteria population; (c) Vaccinated population; (d) Recovered population.

3.8 Endemic equilibrium point global stability

Theorem 3.7: The point E^* is globally asymptotically stable if $R_{Eff} > 1$, otherwise unstable.

Proof: We construct the Lyapunov function given by

$$L = (S - S^* - S^* \ln \frac{S}{S^*}) + (V - V^* - V^* \ln \frac{V}{V^*}) + (I - I^* - I^* \ln \frac{I}{I^*}) + \frac{\beta B^* S^*}{\eta I^* (K + B^*)} (B - B^* - B^* \ln \frac{B}{B^*}) \quad (24)$$

Taking the derivative of L in Equation 24 alongside the solutions of equation of model (1) yields

$$\frac{dL}{dt} = \left(1 - \frac{S^*}{S}\right) \frac{dS}{dt} + \left(1 - \frac{V^*}{V}\right) \frac{dV}{dt} + \left(1 - \frac{I^*}{I}\right) \frac{dI}{dt} + \frac{\beta B^* S^*}{\eta I^* (K + B^*)} \left(1 - \frac{B^*}{B}\right) \frac{dB}{dt} \quad (25)$$

At endemic equilibrium steady state, we have

$$\left. \begin{aligned} (1-p)\pi &= -\sigma V^* + \frac{\beta B^*}{K+B^*} S^* + (\delta + \mu) S^* \\ p\pi &= -\delta S^* + \frac{\theta \beta B^*}{K+B^*} V^* + (\sigma + \varphi + \mu) V^* \\ \frac{\frac{\beta B^*}{K+B^*} S^* + \frac{\theta \beta B^*}{K+B^*} V^*}{I^*} &= (\varepsilon + \omega + \mu) \\ \mu_b &= \frac{\eta I^*}{B^*} \end{aligned} \right\} \quad (26)$$

Substituting Equation 25 in Equation 26 and simplify

$$\begin{aligned} \left(1 - \frac{S^*}{S}\right) \frac{dS}{dt} &= \left(1 - \frac{S^*}{S}\right) \left[-\sigma V^* + \frac{\beta B^*}{K+B^*} S^* + (\delta + \mu) S^* + \sigma V - \frac{\beta B}{K+B} S - (\delta + \mu) S \right] \\ &\leq \frac{\beta B^* S^*}{K+B^*} \left(1 - \frac{S^*}{S}\right) \left[\left(1 - \frac{BS(K+B^*)}{S^* B^* (K+B)}\right) \right] \\ \left(1 - \frac{V^*}{V}\right) \frac{dV}{dt} &= \left(1 - \frac{V^*}{V}\right) \left[-\delta S^* + \frac{\theta \beta B^*}{K+B^*} V^* + (\sigma + \varphi + \mu) V^* + \delta S - \frac{\theta \beta B}{K+B} V - (\sigma + \varphi + \mu) V \right] \\ &\leq \frac{\theta \beta B^* V^*}{K+B^*} \left(1 - \frac{V^*}{V}\right) \left[\left(1 - \frac{BV(K+B^*)}{B^* V^* (K+B)}\right) \right] \\ \left(1 - \frac{I^*}{I}\right) \frac{dI}{dt} &= \left(1 - \frac{I^*}{I}\right) \left[\frac{\beta B}{K+B} S + \frac{\theta \beta B}{K+B} V - \left(\frac{\beta B^*}{K+B^*} S^* + \frac{\theta \beta B^*}{K+B^*} V^* \right) \frac{I}{I^*} \right] \\ &= \left(1 - \frac{I^*}{I}\right) \left[\frac{\beta B^* S^*}{K+B^*} \left(\frac{BS(K+B^*)}{B^* S^* (K+B)} - \frac{I}{I^*} \right) + \frac{\theta \beta B^* V^*}{K+B^*} \left(\frac{BV(K+B^*)}{B^* V^* (K+B)} - \frac{I}{I^*} \right) \right] \\ \frac{\beta B^* S^*}{\eta I^* (K+B^*)} \left(1 - \frac{B^*}{B}\right) \frac{dB}{dt} &= \frac{\beta B^* S^*}{\eta I^* (K+B^*)} \left(1 - \frac{B}{B^*}\right) \left[\eta I - \frac{\eta I^*}{B^*} B \right] = \frac{\beta B^* S^*}{(K+B^*)} \left(1 + \frac{I}{I^*} - \frac{B}{B^*} - \frac{B^* I}{B I^*} \right) \end{aligned}$$

For the function $\mathcal{L}(x) = 1 - x + \ln x$, we know that $x > 0$ leads to $\mathcal{L}(x) \leq 0$. And if $x = 1$, then $\mathcal{L}(x) = 0$. Note that

$$\begin{aligned} \frac{\beta B^* S^*}{K+B^*} \left(1 - \frac{S^*}{S}\right) \left[\left(1 - \frac{BS(K+B^*)}{S^* B^* (K+B)}\right) \right] + \frac{\beta B^* S^*}{K+B^*} \left(1 - \frac{I^*}{I}\right) \left[\left(\frac{BS(K+B^*)}{B^* S^* (K+B)} - \frac{I}{I^*} \right) \right] &= \frac{\beta B^* S^*}{K+B^*} \left[2 - \frac{S^*}{S} - \frac{I^*}{I} + \frac{B(K+B^*)}{B^* (K+B)} - \frac{BS(K+B^*)}{B^* S^* (K+B)} \frac{I^*}{I} \right] \leq \frac{\beta B^* S^*}{K+B^*} \left[\frac{B}{B^*} - \ln \left(\frac{B}{B^*} \right) - \frac{I}{I^*} + \ln \left(\frac{I}{I^*} \right) \right] \\ &= \frac{\theta \beta B^* V^*}{K+B^*} \left(1 - \frac{V^*}{V}\right) \left[\left(1 - \frac{\theta \beta BV(K+B^*)}{B^* V^* (K+B)}\right) \right] + \frac{\theta \beta B^* V^*}{K+B^*} \left(\frac{BV(K+B^*)}{B^* V^* (K+B)} - \frac{I}{I^*} \right) \leq \frac{\theta \beta B^* V^*}{K+B^*} \left[\frac{B}{B^*} - \ln \left(\frac{B}{B^*} \right) - \frac{I}{I^*} + \ln \left(\frac{I}{I^*} \right) \right] < \frac{\beta B^* V^*}{K+B^*} \left[\frac{B}{B^*} - \ln \left(\frac{B}{B^*} \right) - \frac{I}{I^*} + \ln \left(\frac{I}{I^*} \right) \right] \end{aligned}$$

Since $0 < \theta < 1$.

Moreover,

$$\frac{\beta B^* S^*}{(K+B^*)} \left(1 - \frac{B^*}{B}\right) \left[\frac{I}{I^*} - \frac{B}{B^*} \right] = \frac{\beta B^* S^*}{(K+B^*)} \left(1 + \frac{I}{I^*} - \frac{B}{B^*} - \frac{B^* I}{B I^*} \right) \leq \frac{\beta B^* S^*}{(K+B^*)} \left[\frac{B}{B^*} - \ln \left(\frac{B}{B^*} \right) + \frac{I}{I^*} - \ln \left(\frac{I}{I^*} \right) \right]$$

Therefore, the equation is receded as follows

$$\begin{aligned} \frac{dL}{dt} &\leq \frac{\beta B^* S^*}{K+B^*} \left[\frac{B}{B^*} - \ln \left(\frac{B}{B^*} \right) - \frac{I}{I^*} + \ln \left(\frac{I}{I^*} \right) \right] \\ &+ \frac{\theta \beta B^* V^*}{K+B^*} \left[\frac{B}{B^*} - \ln \left(\frac{B}{B^*} \right) - \frac{I}{I^*} + \ln \left(\frac{I}{I^*} \right) \right] \\ &+ \frac{\beta B^* S^*}{(K+B^*)} \left[\frac{B}{B^*} - \ln \left(\frac{B}{B^*} \right) + \frac{I}{I^*} - \ln \left(\frac{I}{I^*} \right) \right] \leq 0 \quad (27) \end{aligned}$$

This implies that $\frac{dL}{dt} \leq 0$ by arithmetic and geometric means. In addition, $L = 0$ if $V = V^*$, $S = S^*$, $I = I^*$, $R = R^*$, and $B = B^*$. According to LaSalle's [23] variance principle, the endemic equilibrium is globally asymptotically attained whenever $R_{Eff} > 1$.

3.9 Sensitivity analysis

We used the normalized forward sensitivity index definition from Blower and Dowlatabadi [24]; Nyerere et al. [25]; Engida et al. [26] to do sensitivity analysis. The sensitivity index of

$$R_{Eff} = \frac{\beta \eta \pi (\delta \theta + \sigma + \varphi + u) (1-p) + p(\theta (\delta + u) + \sigma)}{k \mu_b (\varepsilon + \omega + \mu) [\mu (\mu + \delta + \varphi + u) + \delta \varphi]}$$

to some of the parameters, for instance

$$\begin{aligned} S_{\beta}^{R_{Eff}} &= \frac{\partial R_0}{\partial \beta} \frac{\beta}{R_0} = \frac{R_0}{\beta} \frac{\beta}{R_0} = 1 > 0 \\ S_{\omega}^{R_{Eff}} &= -\frac{\omega}{(\varepsilon + \omega + \mu)} < 0 \end{aligned}$$

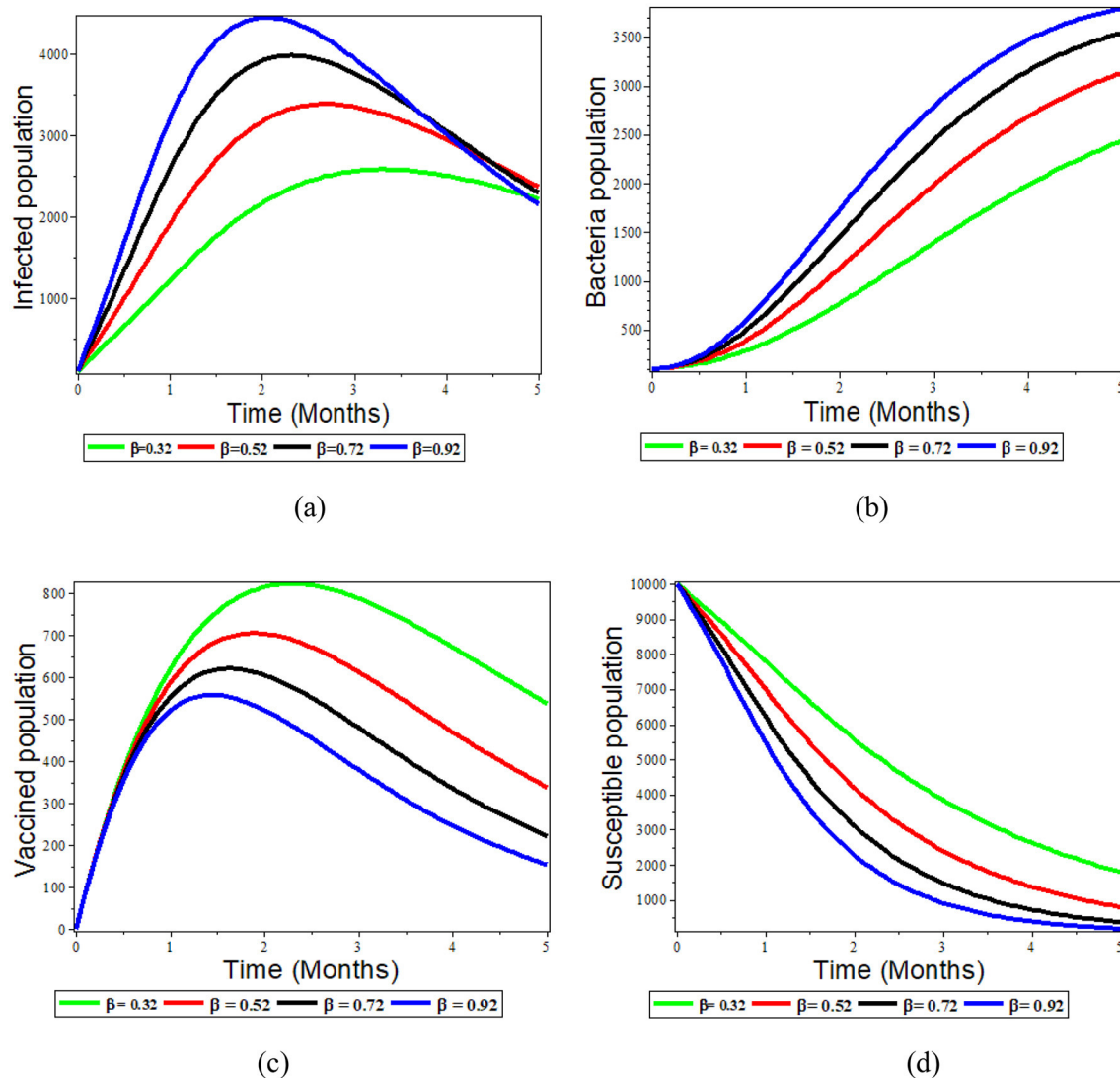


FIGURE 5

Graphs showing the effect of varying β on the population; (a) Infected population; (b) Bacteria population; (c) Vaccinated population; (d) Susceptible population.

$$S_p^{R_{Eff}} = \frac{\beta\eta\pi(\delta(1-p) + p + (\delta + \mu))}{k\mu_b(\varepsilon + \omega + \mu)[\mu(\mu + \delta + \varphi + u) + \delta\varphi]} > 0$$

$$S_p^{R_{Eff}} = - \left(\frac{p(\delta\theta + \mu + \sigma + \varphi) + (\delta\theta + \mu\theta + \sigma)}{(\delta\theta + \mu + \sigma + \varphi)(1-P) + p(\delta\theta + \mu\theta + \sigma)} \right) < 0$$

Similarly, the other parameters are computed and their sensitivity indices are in Table 2.

According to Table 2, the parameters with positive indices (β , θ , σ , ϕ , η , and π) show that, as their values rise, so does the effective reproduction number. If their values are raised, it suggests that they influence the spread of the disease within the population. Furthermore, as their values rise, the factors with negative sensitivity indices (ε , ω , μ , δ , μ_b , K , and p) have an impact on the effective reproduction number, which will lower the endemicity of the bacteria in the population. Figure 2 shows

the reproduction number's sensitivity indices in relation to the basic parameters.

4 Numerical simulation

To show the analytical findings for the proposed model, we conducted a numerical computation [19, 27]. This is carried out using a set of parameter values that are listed in the table below and that in particular come from the literature, together with certain parameter considerations. The Runge-Kutta method of order four was used to execute numerical simulations of the model using the built-in MAPLE function ode45. We considered different initial conditions for the human and bacteria population. The following initial conditions, $S(0) = 10,000$, $I(0) = 100$, $V(0) = 0$, $R(0) = 0$, $B(0) = 10$, with parameters in Table 1 are used for simulation.

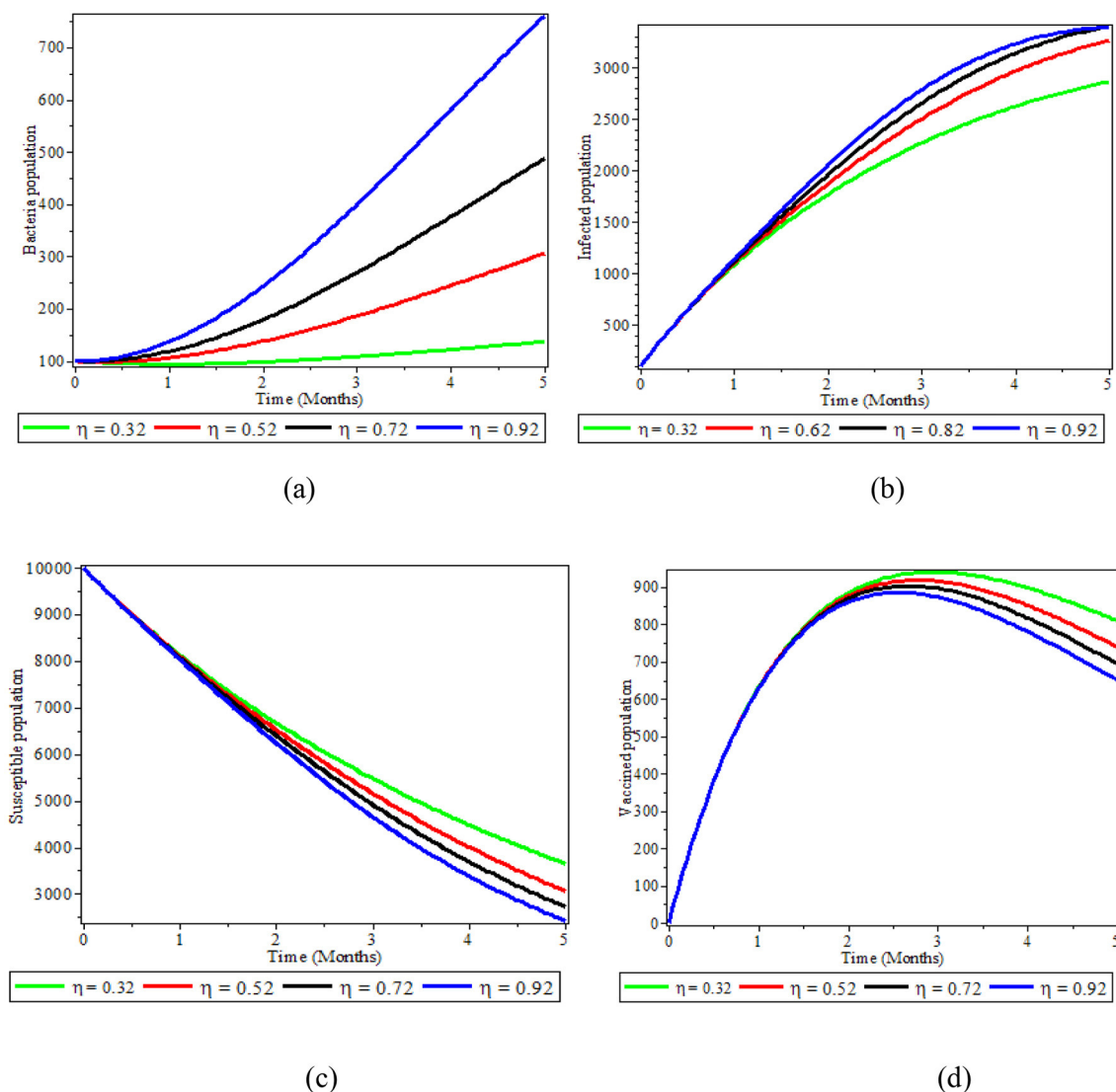


FIGURE 6

Graphs showing the effect of varying η on bacteria population; (a) Bacteria population; (b) Infected population; (c) Susceptible population; (d) Vaccinated population.

4.1 Representation of the model when $R_{\text{Eff}} < 1$ and $R_{\text{Eff}} > 1$

Figure 3a demonstrates the dynamical behavior of bacteria in the environment and susceptible, vaccinated, infected, and recovered subpopulations. Additionally, the period is assumed to be between 0 and 10 months, and the initial population size for the compartmental population susceptible, vaccinated, infected, recovered, and bacteria in the environment is assumed to be respectively 10,000, 100, 0, 0, and 100. The numerical solution is convergent to the DFE point E^0 . It indicates that there are no bacteria in the environment or infected individuals for a long time and shows that there is a disease-free state that is $R_{\text{Eff}} < 1$.

The susceptible and vaccinated populations decline while the number of infected grows, as can be seen in Figure 3b above. Furthermore, the infected population is entirely above the

vaccinated compartment graph and, as time passes, the vaccinated compartment graph approaches the time axis graph. This suggests that the vaccinated population is close to zero and demonstrates the inefficiency of the vaccination. We observed that the disease is endemic when R_{Eff} is greater than one.

4.2 The effect of varying δ and ϕ on the population

Figures 4a–d above illustrates the impact of a combined effect of vaccination rate and vaccine efficiency. One can observe from Figure 4a that these combined effects allow reducing the size of infected individuals, and Figure 4b shows the *S. typhi* bacteria population as the number of vaccinations increases and

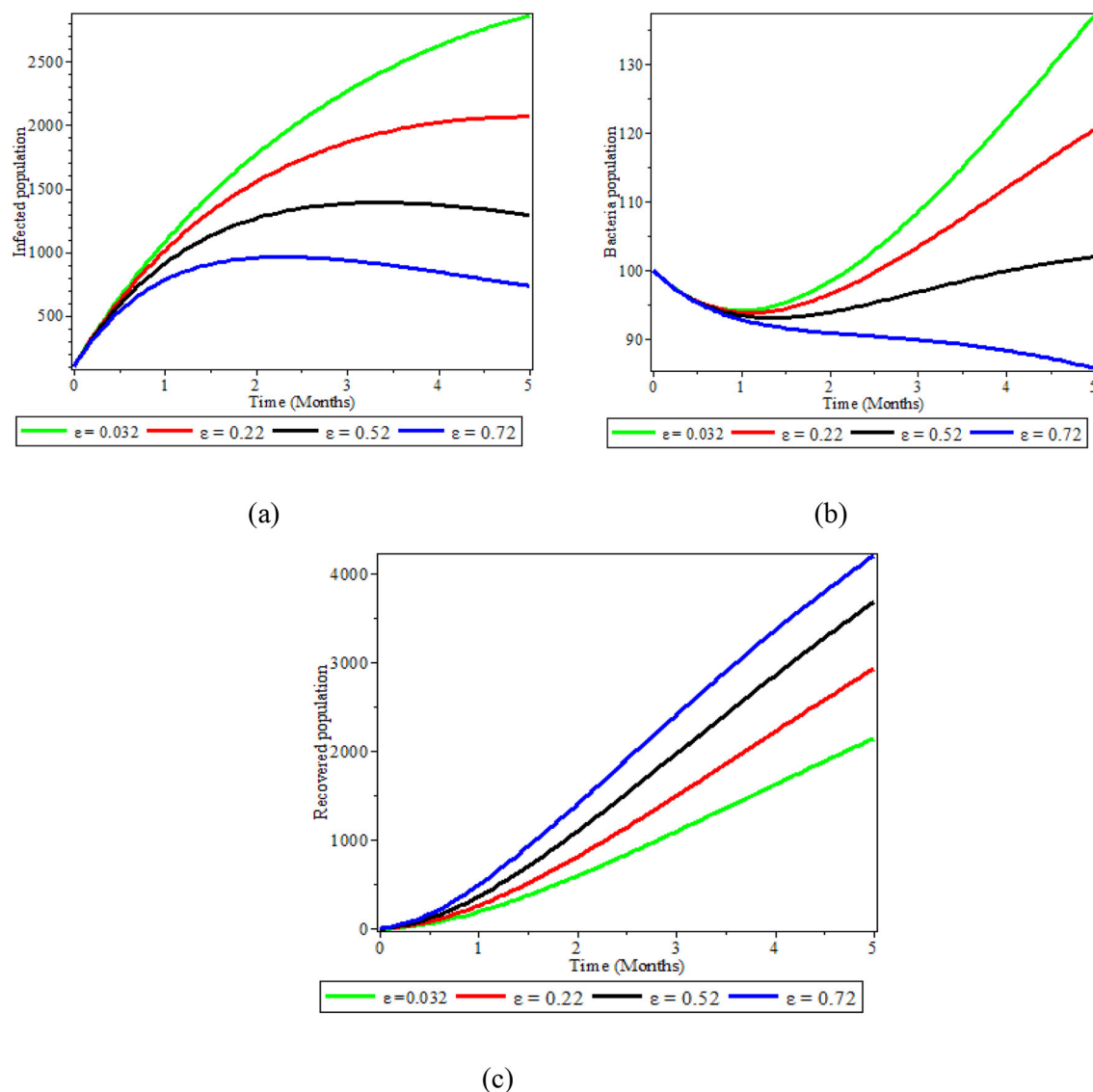


FIGURE 7
Graphs showing the effect of varying ϵ on populations; (a) Infected population; (b) Bacteria population; (c) Recovered population.

its effectiveness become perfect. On the other side, the [Figure 4c](#) vaccine population and [Figure 4d](#) recovered population grow in number as the number of vaccinations increases and its effectiveness become perfect. Thus, a simultaneous increase of the effective vaccination rate and vaccine efficiency greatly reduced the proportion of the infected population. Therefore, boosting and improving the immunization rate as well as increasing the vaccine efficacy is an effective control measure against typhoid.

4.3 The effect of varying β infected population

The ingestion rate of *S. typhi* bacterium population is directly correlated with the disease transmission rate, as shown in [Figures 5a–d](#) below. [Figures 5a, b](#) demonstrate that, as the

ingestion rate mechanisms increases, both the bacterial and infected populations increase.

Although the rate of disease transmission is inversely proportional to the number of susceptible, recovered, and vaccinated individuals, [Figures 5c, d](#) demonstrate that when the rate of ingestion increases, the number of susceptible and vaccinated individuals decreases. Therefore, ingestion rates are thus reduced when efforts are made to expand access to clean water and proper sanitation and hygiene for food handlers.

4.5 The effect of varying η on bacteria population

In this section, we illustrated the effect of varying the parameter value of η while the other parameters are fixed. From [Figure 6a](#), the

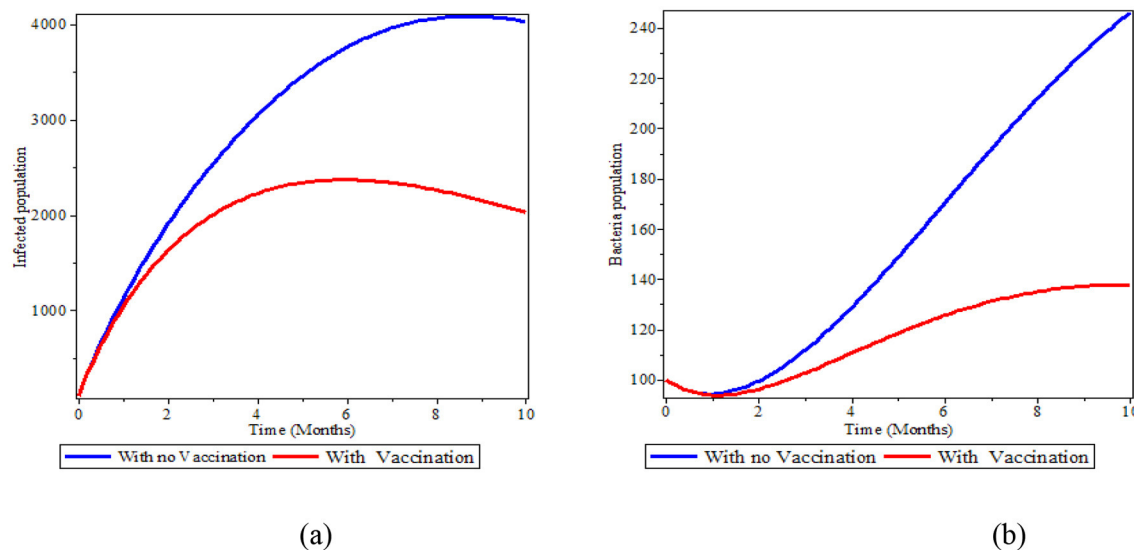


FIGURE 8
The effect of immunization in the infected human and bacteria population; (a) Infected population; (b) Bacteria population.

number of bacteria increases as the infectious individuals increase, contaminating the environment with *S. typhi*. This again leads to an increase in the number of infected people, as is shown in Figure 6b. Conversely, from Figure 6c, increasing the value of η brings a decrease in the number of susceptible people due to the increment infectious individuals and *S. typhi* population. The vaccine population also moves down, as is seen in the Figure 6d. Therefore, we recommend working on strategies to reduce the number of infections contaminating the environment with *S. typhi*, such as avoiding raw fruit and vegetables, peeling fruit yourself, and not eating the peel.

4.6 The effect of varying ϵ on bacteria population

As illustrated in Figures 7a–c, we demonstrated how the recovery of infected individuals affects the populations of bacteria, infected people, and recovered people. When we treat individuals with infections at higher rates with antibiotics and fluids, the number of infectious individuals decreases, as shown in Figure 7a. This leads to an increased number of recovered individuals, as depicted in Figure 7b. As Figure 7c also demonstrates, an increase of treatment to infectious individuals produces a reduction in the number of *S. typhi* bacteria population in the environment. Therefore, treatment of infected individuals is a good strategy that significantly affects bacteria concentration reduction in the environment.

4.7 The effect of immunization on human and bacteria population

Figures 8a, b illustrates the significance of immunization in the population. As illustrated in Figure 8a, the deficiency of vaccination

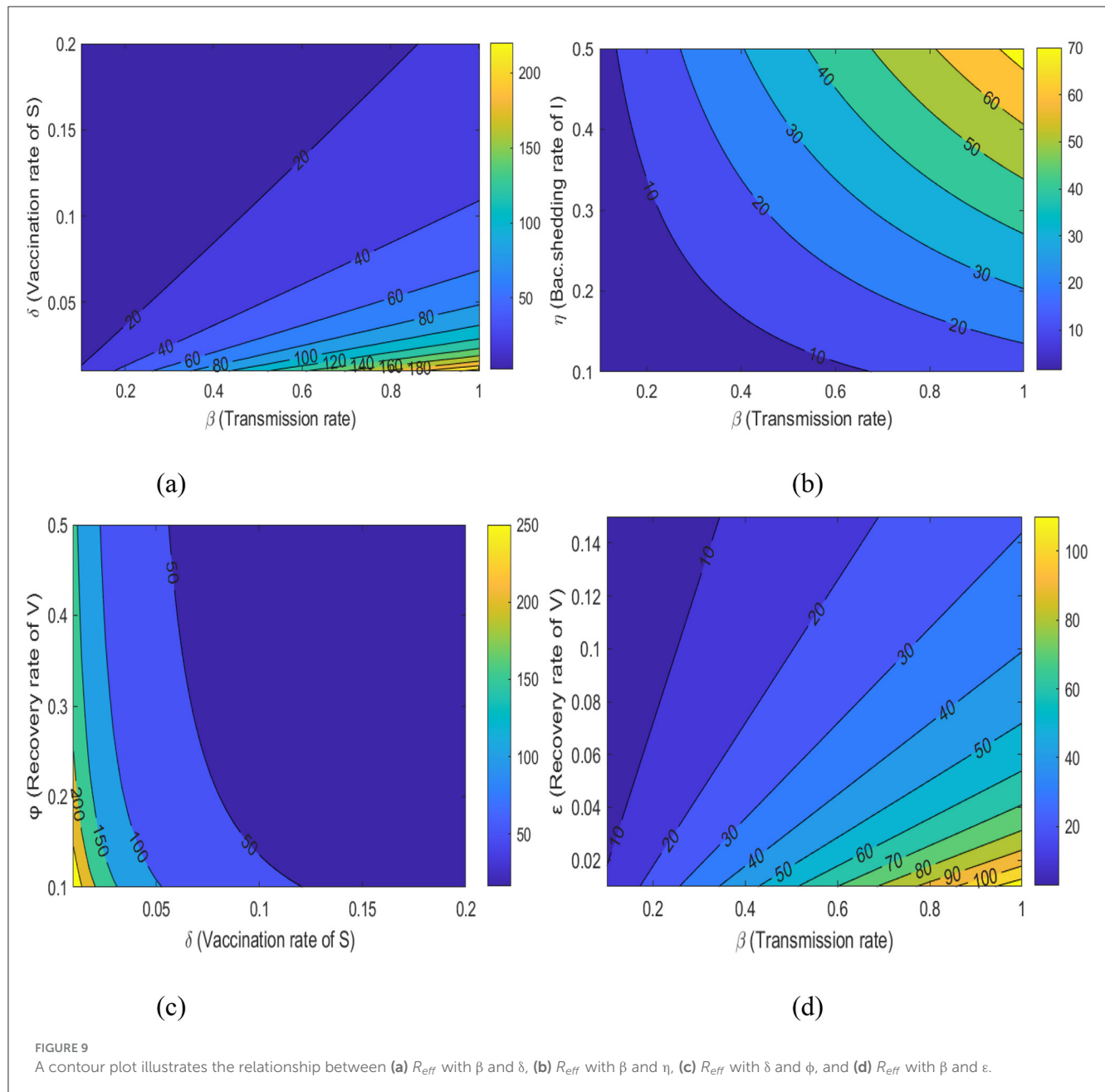
in the population increases the number of infected people and puts the susceptible population at risk of infection; the number of infected individuals drastically drops after the vaccination is made available to the public. We can also observe from Figure 8b that the presence of immunization in the human population reduces the bacteria in the environment. Therefore, people should get vaccinated against typhoid fever before visiting a high-risk area. However, one should still use caution when eating, drinking, and interacting with others because the typhoid vaccine is only 50–80% effective.

The correlation between the R_{eff} and β , ϵ , δ , φ , and η is depicted in Figures 9a–d. Figure 9a illustrates how the vaccination approaches can affect the likelihood of disease transmission within a community. Working on decreasing transmission rate below 0.2 and increasing the immunity label of susceptible individuals above 0.2 decreases the R_{eff} below 20%. Therefore, boosting the vaccination susceptible individuals at a higher rate dramatically lowers R_{eff} , which in turn lowers the probability of an outbreak.

Figure 9b illustrates how variations in the shedding rate of environmental bacteria by infected individuals affects the likelihood of disease transmission within a community. If the disease transmission rate decreased below 0.4 and the shedding rate increased above 0.5, R_{eff} can be reduced below 10%. Therefore, implementing interventions targeting sanitary deficiencies and promoting hygienic practices in the community can lower R_{eff} , which in turn reduces the probability of disease persistence.

Figure 9c also illustrates how the immunity rate of susceptible individuals, and consequently the recovery rate of vaccinated individuals, affects the probability of disease transmission within a community.

Boosting disease vaccination rates above 0.15 and increasing the recovery rate of vaccinated individuals above 0.15 decreases the R_{eff} below 50%. Finally, Figure 9d shows that increasing the recovery rate of vaccinated individuals above 0.15 and reducing the disease transmission rate below 0.2 reduces the R_{eff} below 20%. Therefore, we should work on interventions in the community to



lesser R_{eff} , which in turn lowers the probability of an outbreak of the disease.

5 Results and conclusion

In this work, we studied the dynamics of typhoid fever transmission by taking into consideration *S. typhi* bacteria population in the environment and dividing the people into four subpopulations. After exploring a few mathematical ideas, including boundedness and equilibrium investigation, we estimated the effective reproduction number using the next-generation matrix. Moreover, we evaluated stability and confirmed that the proposed model is asymptotically stable both

locally and globally for both typhoid fever-free equilibrium and endemic equilibrium points. The sensitivity analysis and numerical simulation were presented to show the practical significance of the parameters in the proposed typhoid model. By modifying the model's parameter values, a simulation study and evaluation are carried out. The pictorial representation shows that when the rates of β and η increase, the diseases propagate in the community. On the other side, as the values of the parameters ϵ and δ increase, the disease's ability to replicate diminishes. Typhoid vaccination rates have a substantial effect on the rate of disease transmission. Therefore, improving immunization initiatives is vital for controlling the transmission dynamics of typhoid fever. Additionally, proper disposal of feces and urine should be encouraged, and drinking water from domestic sources should

be boiled or disinfected to eliminate bacteria. Additionally, it is strongly suggested that fruits should be washed with fresh water before consumption. Sanitation food and periodic medical exams should be required.

Data availability statement

The original contributions presented in the study are included in the article/supplementary material, further inquiries can be directed to the corresponding author.

Ethics statement

Ethical approval was not required for the study involving humans in accordance with the local legislation and institutional requirements. Written informed consent to participate in this study was not required from the participants or the participants' legal guardians/next of kin in accordance with the national legislation and the institutional requirements. The manuscript presents research on animals that do not require ethical approval for their study.

Author contributions

HT: Conceptualization, Supervision, Validation, Visualization, Writing – original draft. YZ: Formal analysis, Investigation, Methodology, Writing – original draft. EB: Supervision, Visualization, Writing – review & editing. GT: Conceptualization, Formal analysis, Investigation, Supervision, Writing – review & editing.

References

- Heymann DL. *Control of Communicable Diseases Manual* (No. Ed. 19). American Public Health Association (2008).
- Crump JA, Luby SP, Mintz ED. The global burden of typhoid fever. *Bull World Health Organ.* (2004) 82:346–53.
- Mushayabasa S. A simple epidemiological model for typhoid with saturated incidence rate and treatment effect. *Int J Math Comput Sci.* (2013) 6:688–95. doi: 10.5281/zenodo.1088092
- World Health Organization (WHO). *Salmonella (Non-Typhoidal): World Health Organization.* Geneva (2018).
- Peter OJ, Ibrahim MO, Akinduko OB, Rabi M. Mathematical model for the control of typhoid fever. *IOSR J Math.* (2017) 13:60–6. doi: 10.9790/5728-1304026066
- González-Guzmán J. An epidemiological model for direct and indirect transmission of typhoid fever. *Math Biosci.* (1989) 96:33–46. doi: 10.1016/0025-5564(89)90081-3
- Ashurst JV, Truong J, Woodbury B. *Salmonella typhi*. Florida, FL: StatPearls Publishing (2022).
- Choe K, Whittington D, Lauria DT. The economic benefits of surface water quality improvements in developing countries: a case study of davao, philippines. In: *The Economics of Water Quality*. Davao: Routledge (2019). pp. 371–89.
- Gordon MA, Graham SM, Walsh AL, Wilson L, Phiri A, Molyneux E, et al. Epidemics of invasive *Salmonella enterica* serovar enteritidis and *S. enterica* Serovar typhimurium infection associated with multidrug resistance among adults and children in Malawi. *Clin Infect Dis.* (2008) 46:963–9. doi: 10.1086/529146
- Maurice J. A first step in bringing typhoid fever out of the closet. *Lancet.* (2012) 379:699–700. doi: 10.1016/S0140-6736(12)60294-3
- Chamuchi MN, Sigey JK, Okello JA, Okwoyo JM. SIICR model and simulation of the effects of carriers on the transmission dynamics of typhoid fever in kisii town kenya. *SIJ Trans Comput Sci Eng Appl.* (2014) 2:109–16. doi: 10.9756/SIJCSEA/V2I4/0203250101
- Akinyi OC, Mugisha JYT, Manyonge A, Ouma C, Maseno K. A model on the impact of treating typhoid with antimalarial: dynamics of malaria concurrent and co-infection with typhoid. *Int J Math Anal.* (2015) 9:541–51. doi: 10.12988/ijma.2015.412403
- Edward S, Nyerere N. Modelling typhoid fever with education, vaccination and treatment. *Eng Math.* (2016) 1:44–52. doi: 10.11648/j.ijtam.20160202.30
- Karunditu JW, Kimathi G, Osman S. Mathematical modeling of typhoid fever disease incorporating unprotected humans in the spread dynamics. *J Adv Math Comput Sci.* (2019) 32:1–11. doi: 10.9734/jamcs/2019/v32i330144
- Wameko M, Koya P, Wodajo A. Mathematical model for transmission dynamics of typhoid fever with optimal control strategies. *Int J Indus Math.* (2020) 12:28396.
- Nyaberi HO, Musaili JS. Mathematical modeling of the impact of treatment on the dynamics of typhoid. *J Egypt Math Soc.* (2021) 29:1–11. doi: 10.1186/s42787-021-00125-8
- Jan R, Boulaaras S, Alnegga M, Abdullah FA. Fractional-calculus analysis of the dynamics of typhoid fever with the effect of vaccination and carriers. *Int J Numer Model Electron Netw Devices Fields.* (2024) 37:e3184. doi: 10.1002/jnm.3184

Funding

The author(s) declare that no financial support was received for the research and/or publication of this article.

Acknowledgments

Our sincere gratitude goes out to the reviewers of the research paper.

Conflict of interest

The authors declare that the research was conducted in the absence of any commercial or financial relationships that could be construed as a potential conflict of interest.

Generative AI statement

The author(s) declare that no Gen AI was used in the creation of this manuscript.

Publisher's note

All claims expressed in this article are solely those of the authors and do not necessarily represent those of their affiliated organizations, or those of the publisher, the editors and the reviewers. Any product that may be evaluated in this article, or claim that may be made by its manufacturer, is not guaranteed or endorsed by the publisher.

18. Van den Driessche P, Watmough J. Reproduction numbers and sub-threshold endemic equilibria for compartmental models of disease transmission. *Math Biosci.* (2002) 180:2948. doi: 10.1016/S0025-5564(02)00108-6
19. Simorangkir G, Aldila D, Rizka A, Tasman H, Nugraha ES. Mathematical model of tuberculosis considering observed treatment and vaccination interventions. *J Interdiscip Math.* (2021) 24:1717–37. doi: 10.1080/09720502.2021.1958515
20. Castillo-Chavez C, Song B. Dynamical models of tuberculosis and their applications. *Math Biosci Eng.* (2004) 1:361. doi: 10.3934/mbe.2004.1.361
21. Alemneh HT, Alemu NY. Mathematical modeling with optimal control analysis of social media addiction. *Infect Dis Model.* (2021) 6:405–19. doi: 10.1016/j.idm.2021.01.011
22. Tilahun GT, Alemneh HT. Mathematical modeling and optimal control analysis of COVID-19 in Ethiopia. *J Interdiscip Math.* (2021) 24:2101–20. doi: 10.1080/09720502.2021.1874086
23. La Salle JP. *The Stability of Dynamical Systems.* Pennsylvania: Society for Industrial and Applied Mathematics (1976). doi: 10.1137/1.9781611970432
24. Blower SM, Dowlatabadi H. Sensitivity and uncertainty analysis of complex models of disease transmission: an HIV model, as an example. *International Statistical Review/Revue Internationale de Statistique.* (1994) 62:229–43. doi: 10.2307/1403510
25. Nyerere N, Mpeshe SC, Edward S. Modeling the impact of screening and treatment on the dynamics of typhoid fever. *World J Model Simul.* (2018) 14:298–306.
26. Engida HA, Theuri DM, Gathungu D, Gachohi J, Alemneh HT. A mathematical model analysis for the transmission dynamics of leptospirosis disease in human and rodent populations. *Comput Math Methods Med.* (2022) 2022:1806585. doi: 10.1155/2022/1806585
27. Alemneh HT, Makinde OD, Theuri DM. Eco-epidemiological model and analysis of msv disease transmission dynamics in maize plant. *Int J Math Math Sci.* (2019) 24:7965232. doi: 10.1155/2019/7965232